J Clust Sci (2017) 28:607–619
DOI 10.1007/s10876-016-1141-5

ORIGINAL PAPER

Enhanced Antibacterial and Cytotoxic Activity of Phytochemical Loaded-Silver Nanoparticles Using *Curculigo orchioides* Leaf Extracts with Different Extraction Techniques

Perumal Venkatachalam[1] · Thamilchelvan Kayalvizhi[1] · Jinu Udayabanu[1] · Giovanni Benelli[2] · Natesan Geetha[3]

Received: 25 November 2016 / Published online: 31 January 2017

Abstract Green synthesis of nano-materials is attracting high research attention nowadays, due to its eco-friendly features. This study describes an efficient method for green synthesis of silver nanoparticles (AgNPs) by two extraction techniques (boiling-CoBLE and grinding-CoGLE) using the leaf extracts of *Curculigo orchioides* Gaetrn. Then, we evaluated their antibacterial activity and cytotoxicity on Henrietta Lacks (HeLa) cells. The synthesized AgNPs were characterized by peaks at 433 nm (CoBLE) and 443 nm (CoGLE) in UV–Visible spectroscopy. X-ray diffraction (XRD) analysis confirmed the crystalline structure of metallic silver ions. The Fourier transform infrared (FTIR) spectroscopy indicated the presence of various bioactive compounds with –OH functional groups that might act as capping and stabilizing agent for nano-synthesis. Field emission scanning electron microscopy (FESEM) and high resolution transmission electron microscopy (HRTEM) suggested that AgNPs were spherical in morphology, with smooth edges and size ranging from 5 to 17 nm. The maximum zone of growth inhibition was observed for CoBLENPs against *Pseudomonas aeruginosa* (18 mm) and *Staphylococcus aureus* (14 mm). Cytotoxicity of AgNPs was determined and the inhibitory concentration (IC_{50}) was 6.33 and 57.53 μg/mL for HeLa and Vero cell lines, respectively. Overall, our results suggest that AgNPs synthesized using the leaf extracts of *C. orchioides* may represent a promising source of nano-drugs for cancer therapy in near future.

✉ Perumal Venkatachalam
pvenkat67@yahoo.com

[1] Genetic Engineering and Molecular Biology Lab, Department of Biotechnology Periyar University, Periyar Palkalai Nagar, Salem, Tamil Nadu 636 011, India

[2] Department of Agriculture, Food and Environment, University of Pisa, Via Del Borghetto 80, 56124 Pisa, Italy

[3] Department of Botany, Bharathiar University, Coimbatore, Tamil Nadu 641 046, India

Keywords Cancer therapy · *Curculigo orchioides* · Nanoparticles · Microbial pathogens

Introduction

Currently, there is an increasing commercial demand for nanoparticles due to their wide applicability in various fields, including medicine, catalysis, electronics, chemistry, agriculture and veterinary [1]. Over the last two decades, chemical reduction, electrochemical techniques, and photochemical reduction modes of synthesizing silver nanoparticles (AgNPs) with the addition of some chemical reductants, such as borohydride, citrate, ascorbate and elemental hydrogen, have been used [2–4]. However, the reagents used in the synthesis of AgNPs may not be eco-friendly and can pollute the environment [5]. To overcome these limitations, researchers are now focusing on "green synthesis" of AgNPs using plant-based reducing agents as more environmentally friendly, less toxic, and cheaper mode of synthesis compared to the physical and chemical modes [6]. Natural phytochemicals from plants have been extracted and applied for extracellular production of metallic silver nanoparticles that showed effective antibacterial, anticancer and larvicidal activity [7, 8].

Curculigo orchioides, belonging to the family Hypoxidaceae, is a flowering plant species in the genus *Curculigo* found all over India, especially in sandy areas of hotter regions. In the traditional medicine system (*Unani*), the leaves of *C. orchioides* have been reported to have anticancer properties. In most Ayurvedic formulations, the rhizomes of *C. orchioides* are extensively used as a substitute for "*safed musli*". These formulations are reputed to act as a demulcent, diuretic, aromatic tonic, and aphrodisiac, in the treatment of leprosy and nervous diseases. The antimicrobial activity of the extract of *C. orchioides* has also been reported [9]. The in vitro cytotoxic and anticancer activities of the rhizome extract of *C. orchioides* against the human larynx epithelial carcinoma cell line (Hep_2) have also already been noted [10].

C. orchioides rhizome extracts prepared by using different solvents showed antitumor activity against human breast cancer cells MCF-7 [11]. Recently, plant-mediated metal nanoparticles were tested for their anticancer activity on human cervical carcinoma cells. More generally, Ag metal plays a prominent role in that anticancer activity compared to other metal nanoparticles obtained through plant extracts [12].

Silver is well known as one of the most universal antimicrobial substances that exhibits a low toxicity in humans and has diverse in vitro and in vivo applications with broad-spectrum antimicrobial activity against human and animal pathogens. Additionally, silver is now added into commercial, medical and consumer products [13, 14]. Cervical cancer is one of the few cancers that affects young women, and thus, the death rate due to this disease has been dramatically increasing worldwide [15]. The current therapeutic approaches toward cancer include surgery, chemotherapy and radiotherapy [16]. Major disadvantage of the application of chemical anti-

cancer drugs are represented by severe side-effects, including hair loss, fever, diarrhea, nausea, joint pain, anemia, cardiotoxicity, reduced fertility, sexual problems and dry skin [17]. The development of anticancer drugs with fewer side effects and better therapeutic efficacy remains one of the most challenging areas in cancer treatment [18]. Therefore, an environmentally friendly reducing agent and a nontoxic stabilizing agent with phytochemical-mediated AgNPs will be an alternative with added medical advantages.

Hence, the present study is mainly focused on the synthesis and characterization of phytochemicals loaded-AgNPs using aqueous leaf extracts (direct boiling and grinding) of *C. orchioides*. The synthesized AgNPs were assessed for their antibacterial and anticancer activities against human microbial pathogens and cervical cancer cells (HeLa), respectively.

Materials and Methods

Plant Material

Seedlings of *C. orchioides* Gaetrn. were maintained in the Green House of Periyar University, Tamil Nadu, India. Silver nitrate ($AgNO_3$) of analytical grade was purchased from SRL Chemicals Pvt. Limited (Mumbai, India). Muller Hinton Agar was obtained from Hi-Media Laboratories Pvt. Limited (Mumbai, India). The remaining chemicals and reagents were of analytical grade.

Preparation of Aqueous Leaf Broth

Healthy and fresh leaves of *C. orchioides* were collected and washed with copious amounts of sterile nanopure water (conductivity = 18 μΩ/m, TOC <3 ppb; Barnstead, Waltham, MA, USA). The aqueous solutions of the leaves were prepared by the following two techniques: one is boiling the leaves directly with nanopure water, and the second is grinding the leaves with nanopure water followed by centrifugation to obtain an aqueous broth. Five grams of *C. orchioides* leaves were chopped and boiled for 10 min at 60 °C in 25 mL of nanopure water followed by filtration using Whatman No. 1 filter paper, and this leaf broth is referred to as CoBLe. The same amount of leaves was ground well using a mortar and pestle with 25 mL of nanopure water followed by centrifugation at 10000 rpm for 10 min to obtain an aqueous broth (CoGLe).

Biological Synthesis of AgNPs with CoBLe and CoGLe Leaf Broths

Approximately 25 mL of CoBLe and CoGLe broths were mixed separately with 225 mL of $AgNO_3$ (5 mM) solution, and the reaction mixtures were incubated at room temperature for 5 h. Light yellowish color of the mixture turned to a brown color with a yellow shade indicating the formation of AgNPs, whereas the control solution remains unchanged. Furthermore, the reaction mixtures were centrifuged at

8000 rpm for 10 min. Pellets obtained were completely suspended in double distilled water and centrifuged 3×. Pellets contained in the suspension were separately transferred into a glass petri dish and dried in an oven overnight at 60 °C.

Bio-physical Characterization of the AgNPs

The optical properties of samples were periodically analyzed using an UV–Visible spectrophotometer (Systronics UV 2203, Ahmedabad-382330, Gujarat, India) within a working wavelength range of 300–650 nm using a dual beam operating at 1 nm resolution. The obtained powder of NPs was analyzed using an advanced power X-ray diffractometer (XRD; Rigaku, Mini Flex II, Japan) operated at a voltage of 9 kW and a current of mA with CuKα radiation. Fourier transform infrared spectroscopy (FTIR; Perklin Elmer, Spectrum RX I) characterization was carried out to obtain information about the functional groups present in the AgNPs by scanning them in the range of 400–4000 cm^{-1} at a resolution of 4 cm^{-1} in KBr pellets. For the morphological analysis of the prepared nanostructured samples, field emission scanning electron microscopy (FESEM, Carl Zeiss, SUPRA55 model) with energy dispersive X-ray (EDX) analysis was performed to determine the surface inter-atomic distribution and presence of elemental silver. The average particle size of the prepared AgNPs was determined using the Sigma ScanPro software. High-resolution transmission electron microscopy (HRTEM; JEOL, JEM 2100, Japan) along with selected area electron diffraction (SAED) pattern was used to visualize the size and shape of the nanoparticles as well as to reveal the crystalline nature of the AgNPs for both modes of preparation.

Antibacterial Activity of Phytomolecule Loaded-AgNPs

In vitro antibacterial activities of the AgNPs synthesized by the two different methods were evaluated by the agar well diffusion method using clinically isolated Gram negative microorganisms, including *Escherichia coli, Klebsiella pneumoniae,* and *Pseudomonas aeruginosa*, as well as the Gram positive microorganism *Staphylococcus aureus*. Cultures were grown on nutrient broth at 37 °C for 24 h. The concentration of the microbial inoculums was adjusted to 2.5×10^5 colony-forming units (CFU) per mL as measured with the McFarland turbidity standard using a spectrophotometer at 600 nm. The standardized cultures were swabbed on Muller-Hinton agar with sterile cotton swabs, and approximately 6-mm wells were made with help of gel punctures. Each well was loaded with 50 μL of CoBLe-AgNPs, CoGLe-AgNPs, $AgNO_3$, CoBLe/GLe and the antibiotic ciprofloxacin followed by incubation at 37 °C for 24 h. Then, the inhibition zones were measured. The study was performed at SKS Hospital Laboratory Services, Salem, which is accredited with a certificate from the National Accreditation Board for Testing and Calibration Laboratories (NABL), New Delhi, India, and it was approved by the Institutional Ethical Committee.

In Vitro Cytotoxicity Studies

HeLa cervical cancer cell line was obtained from National Center for Cell Science (NCCS), Pune, India. The cells were cultured in RPMI1640 medium supplemented with 10% fetal bovine serum from HiMedia along with 100 U/mL penicillin and 100 μg/mL streptomycin (GIBCO). Routinely, the cells were maintained under 95% air and 5% CO_2 in a biological incubator at 37 °C. All of the cell culture procedures were performed in a laminar flow cabinet containing a UV light. Once the cells reached 70–80% confluence, they were ready for the assay. The cell numbers were determined with a hemocytometer, and the cell viability was assessed using MTT assay.

The plates were subjected to MTT assay according to the method previously described, and the percentage of cell viability was determined spectrophotometrically at 570 nm [7, 36]. HeLa cells were cultured and seeded into 96-well plates at a density of approximately 1×10^4 cells/100 μL of medium in each well and incubated in a 5% CO_2 incubator for 24 h. HeLa cells were treated with a series of 100, 10, 1.0, 0.1 and 0.01 μg/mL concentrations of AgNPs synthesized by both modes dissolved in DMSO, and a cell control of DMSO alone was also used. A yellow tetrazole, MTT (3-(4,5-dimethylthiazol-2-yl)-2,5-diphenyl tetrazolium bromide), was prepared in a 5 mg/mL concentration in phosphate-buffered saline, and the plates were incubated for 2 h and 30 min. Fifty microliters of MTT was added into each well, followed by incubation for 48 h. The formed MTT-formazan product (in a crystalline form, formed by mitochondrial dehydrogenase) was dissolved in 100 μL of DMSO after discarding the supernatant, and the amount was estimated by measuring the absorbance using a Synergy H4 microplate reader at 570 nm. The growth percentage was calculated using the following formula:

$$\text{Percentage growth} = 100 \times ((T - T_0)/(C - T_0))$$

where T is the optical density of the test sample, C is the optical density of the control, and T_0 is the optical density at time zero. After 48 h of incubation, the cells were observed under an inverted microscope for the detection of morphological changes and were photographed.

Acridine Orange (AO) and Ethidium Bromide (EtBr) Staining

Approximately 5 μL of the dye mixture (100 mg/mL acridine orange (AO) and 100 mg/mL ethidium bromide (EtBr) in phosphate buffered saline (PBS) was mixed with 9 mL of cell suspension (1×10^5 cells/mL) on clean microscopic cover slips. Cancer cells were collected, washed with PBS (pH = 7.2) and stained with 1 mL of AO/EtBr. After incubation for 2–3 min, the cells were visualized under a fluorescence microscope (Nikon Eclipse, Inc., Japan) at 40× magnification with an excitation filter set at 480 nm. The percentage of apoptotic cells was determined by the following formula:

$$\text{Percentage of apoptotic cells} = \frac{\text{Total number of apoptotic cells}}{\text{Total number of normal and apoptotic cells}} \times 100$$

.

Data Analysis

Each experiment was repeated at least three times, and the standard error was calculated. The data were analyzed using one-way ANOVA with Dunnett's post hoc test using Graph Pad InStat and Prism version 3.00 for Windows, Graph Pad Software, San Diego, CA, USA.

Results and Discussion

Characterization of AgNPs Synthesized by Various Methods

The surface Plasmon resonance (SPR) absorbance of the AgNPs related to 433 nm and 443 nm for CoBLe and CoGLe, respectively (Fig. 1), was measured. The acquired peaks correlated well with earlier studies, including the synthesis of AgNPs using banana peel extract or *Tinospora Crispa* [19, 20]. The variation in the peaks may be due to the concentration of phytochemicals obtained through the two different modes of extraction. The SPR absorbance was extremely sensitive to the size and shape of the NPs, their inter-particle distances and the surrounding media. Variations in the biological material and metal salt concentration are known to influence NP synthesis [2]. According to Velmurugan et al. [5, 21, 22] various phytochemicals present in the leaf extract could play a key role in the conversion of the ionic form of silver to the metallic nano-form.

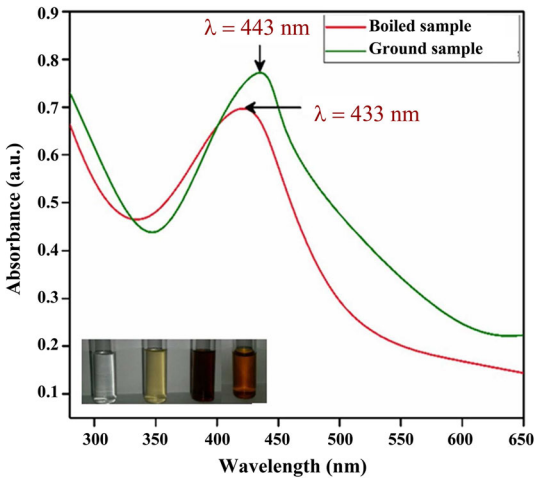

Fig. 1 UV–Visible absorption spectra of AgNPs synthesized using boiled and ground *C. orchioides* leaf extract samples

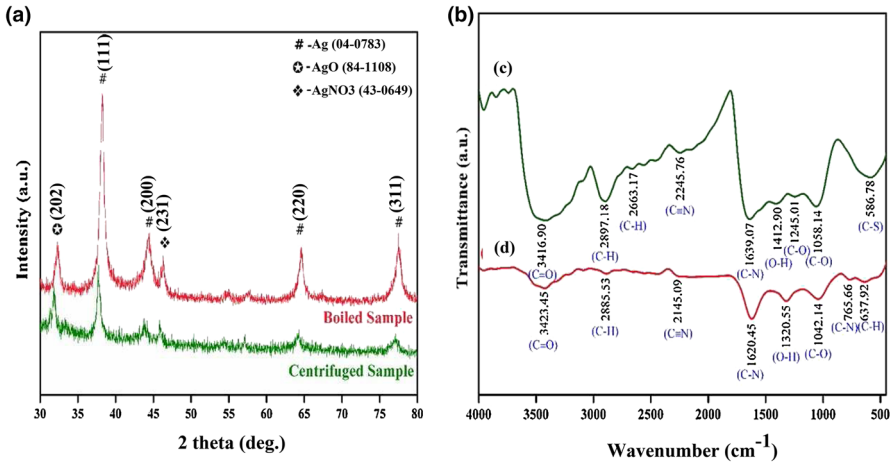

Fig. 2 **a** XRD patterns of samples with direct leaf boiling and **b** direct leaf grinding. **c** FTIR spectra of (**a**) boiled and **b** ground leaf extract-mediated AgNPs

The XRD patterns of CoBLe and CoGLe synthesized AgNPs are shown in Fig. 2a, b. Diffraction peaks at $2\theta = 27.88$, 32.32, 38.17, 47.60 and 27.85, 32.29, 46.32 correspond to (210), (122), (123), (231) and (210), (122), (231) for CoBLe (Fig. 2a) and CoGLe (Fig. 2b), respectively, which indicates that the AgNPs had a cubic crystal structure (Joint Committee on Powder Diffraction Standards; JCPDS no. 43641). In other words, the obtained Ag NPs were crystalline in nature. Our results are in accordance with an earlier report on the synthesis of AgNPs utilizing the surfactant properties of the plant extract when using banana peel extract [19].

FTIR characterization was carried out to identify the possible functional groups present in CoBLe- and CoGLe-mediated synthesized AgNPs. Results are shown in Fig. 2c, d. The broad peaks with deformation in the fingerprint region of 637–3423 cm^{-1} for the AgNPs raised from CoBLe (Fig. 2c), –OH stretching at 1320 cm^{-1}; amide C–N stretching at 1620 cm^{-1}; alkene/aldehyde C–H stretching at 2885 cm^{-1}; and weaker bands at 637 and 3423 cm^{-1} corresponding to alkene group and ketone group stretching, respectively, were found. Therefore, FTIR analysis showed the presence of the OH-group present in the saponin (glycoside) of CoBLe-mediated AgNPs at 1320 cm^{-1}, which may be responsible for the capping and stabilization of AgNPs. Predominant peaks were found in the fingerprint region (586–3416 cm^{-1}) for the AgNPs raised from CoGLe (Fig. 2d). The stretching peaks at 1058 and 1639 cm^{-1} were identified as being due to alkenes and amides of mononuclear benzene rings and vinyl groups as well as citric-substituted functional groups. The intense peak at 2897 cm^{-1} corresponds to alkynes (Fig. 2d). Among these peaks, the stretch at 2245 cm^{-1} is due to a nitrile group, which is a phenolic derivative from CoGLe [23]. Our results were accordance with those previously reported for the synthesis of AgNPs using *Achyranthes aspera* [24], *Memecylon edule* [25], and *Memecylon umbellatum* [26], and the stretch at 2245 cm^{-1} was due to a phenolic derivative present in the *C. orchioides* leaf extract [27], which was found to be responsible for the capping and stabilization of AgNPs synthesized from CoGLe.

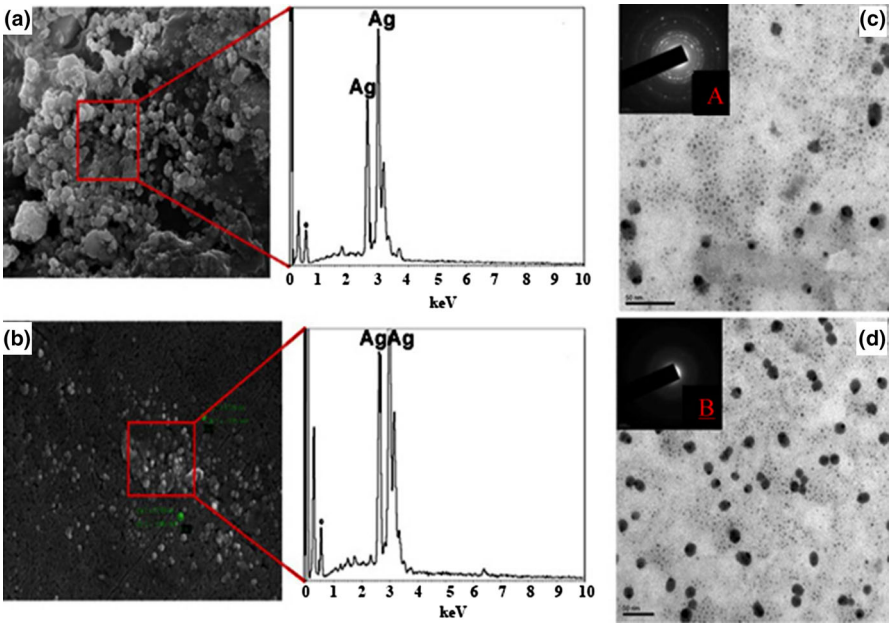

Fig. 3 FESEM and EDAX images of **a** boiled leaf extract and **b** ground leaf extract. HRTEM images of the **c** boiled sample (A-insert, SAED) and **d** grinded sample (B-insert, SAED) of leaf extract-mediated AgNPs

The surface morphologies of the CoBLe- and CoGLe-mediated synthesized AgNPs were visualized by FESEM (Fig. 3a, b). We highlighted a remarkable difference in the surfaces of the AgNPs obtained by CoBLe (Fig. 3a) and CoGLe (Fig. 3b), and the aggregation of particles was observed. This aggregation may be due to the presence of secondary metabolites in the leaf extracts [21, 22, 28]. The EDX profiles for the AgNPs obtained from CoBLe and CoGLe showed strong Ag signals from silver atoms with weak oxygen peaks, which were the two peaks located between 2.5 keV and 3 keV. Both EDX spectra showed the co-existence of AgNPs in smaller and larger sizes due to the formation of AgNPs in early and later stages of the reaction, indicating that the formation of new NPs and aggregation to form larger particles occurred sequentially. The EDX profiles showed some weaker signals for carbon, oxygen and chloride, which were produced from biomolecules of CoBLe and CoGLe. Our findings are comparable to those concerning synthesis relying to *M. umbellatum* leaf extract reported by Arunachalam et al. [26] and *Cassia auriculata* extract-based route reported by Kumar et al. [29].

The morphologies and sizes of the CoBLe- and CoGLe-mediated AgNPs were determined by TEM as shown in Fig. 3c, d, respectively. Most of the particles had uniform spherical morphologies and smooth edges with average sizes of 5–17 nm for CoBLe (Fig. 3c) and 12–20 nm for CoGLe (Fig. 3d). The nanoparticles obtained are highly crystalline, as shown by clear lattice fringes and the SAED patterns shown in the insert pictures of Fig. 3c, d. This high crystallinity is possibly due to the higher concentrations of the reducing agent induced faster nucleation rates that resulted in smaller particle sizes [30]. Based on this, the interface between the surface and the

biomolecules secreted by the leaf materials was very strong and leads to crystal growth prejudiced by the inhibition of silver atom accumulation at the surface [31].

In Vitro Antibacterial Activity of the AgNPs

Nanoparticle growth inhibition activity is presented in Table 1, and a related image is shown in Fig. 4a. AgNPs showed good activities against *P. aeruginosa* (18.6 and 16.3 mm) and *S. aureus* (14.0 and 13.3 mm), with lower activities towards *E. coli* (8.33 and 6.3 mm) and *K. pneumoniae* (8.66 and 12.6 mm) when treated with CoBLe- and CoGLe-derived AgNPs, respectively. The CoBLE-AgNPs showed enhanced inhibition zones against clinical pathogens when compared with the CoGLe-AgNPs, $AgNO_3$ and plant leaf extracts. Ag ions or salts have only limited usefulness as antimicrobial agents due to the interfering effects of salts and the discontinuous release of inadequate concentrations of Ag^+ from the metal [5, 32]. It has been reported that AgNPs interact with bacterial membrane proteins and DNA at preferential sites, as they have a high affinity towards sulfur and phosphorous compounds [33]. This interaction leads to the disruption of the cell membrane, increasing the cell permeability and DNA damage, which leads to cell death and the inhibition of bacterial growth [34].

Moreover, highly reactive metal oxide nanoparticles exhibit excellent bactericidal action against Gram-positive and Gram-negative bacteria [35]. In general, Ag^+ from AgNPs are believed to become attached to the negatively charged bacterial cell wall and rupture it, which leads to the denaturation of protein and finally cell death [5]. AgNPs are small in size so they easily enter into the bacterial cells and affect the intracellular processes such as DNA, RNA and protein synthesis [5, 36].

Determination of the Cytotoxic Effect of AgNPs

Our AgNPs were cytotoxic on HeLa cells at low concentrations. The requirement of 6.33 μg/mL was adequate to achieve 50% inhibition of the biological activity of cancer cells (IC_{50}), as shown in Fig. 4b. At the lowest tested concentration (0.01 μg/mL), CoBLe-AgNPs were able to inhibit the growth of the cell line by less than 5%. Meanwhile, when HeLa cells were treated with 100 μg/mL of AgNPs, they

Table 1 Antimicrobial activity of CoBLe, CoGLe fabricated AgNPs, Co extract, bulk metal and control antibiotic

Clinical pathogen	Co extract (Mean ± SE)	Ciprofloxacin (Mean ± SE)	$AgNO_3$ (Mean ± SE)	CoBLe-AgNPs (Mean ± SE)	CoGLe-AgNPs (Mean ± SE)
E. coli	6.0 ± 0.1^a	13.3 ± 1.2^c	10.0 ± 1.15^c	8.33 ± 0.88^c	6.3 ± 0.33^c
P. aeruginosa	6.6 ± 0.33^a	36.3 ± 1.8^b	19.3 ± 0.66^a	18.6 ± 0.88^a	16.3 ± 0.66^a
S. aureus	6.0 ± 0.11^a	33.3 ± 3.2^b	19.0 ± 1.00^a	14.0 ± 0.57^b	13.3 ± 0.33^b
K. pneumoniae	6.6 ± 0.33^a	40.0 ± 1.5^a	18.0 ± 0.57^b	8.66 ± 1.20^c	12.6 ± 0.88^b

Data represent mean ± SE

Mean values within the column followed by the same letter in superscript are not significantly different at $P < 0.05$ level

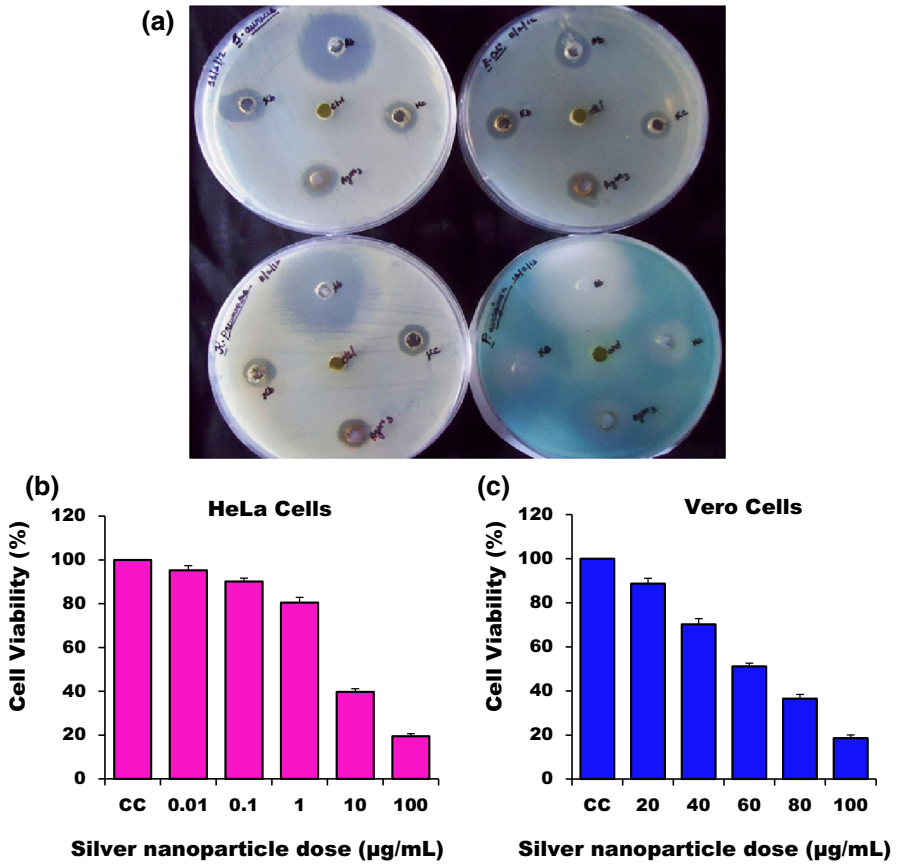

Fig. 4 **a** Photographs of the antimicrobial activity of CoBLe-synthesized AgNPs. MTT assay results confirming the in vitro cytotoxicity of CoBLe-AgNPs on: **b** HeLa cells (*CC* cell control) and **c** Vero cells (*CC* cell control)

significantly inhibited the growth of the cell line with an IC_{50} value of 6.33 µg/mL. In the case of CoBLe-AgNPs, treatment with Vero cells showed an IC_{50} value of 57.53 µg/mL (Fig. 4c). The cell death data obtained in this study allow us to predict the potential of the AgNPs as cytotoxic and anti-tumor agents. Previously, the antitumor activity of the methanolic extract of *C. orchioides* was reported against a breast cancer cell line (MCF-7) [37]. The toxicity of the methanolic extract of *C. orchioides* on the Hep2 cell line, which was nontoxic up to 800 µg/mL, was reported by [38]. In addition, the aqueous extract of the close-related species *C. pilosa* was reported as cytotoxic on HeLa cells with a relative cell death of 70% at 8000 µg/mL [39]. Based on these studies, it is clear that the CoBLe-AgNPs were able to inhibit the growth of HeLa cells at a minimum concentration, and this is the first report of the application of *C. orchioides*-derived NPs on cancerous cells.

The most recognizable changes, such as cell shrinkage, membrane blabbing and apoptotic body formation, due to treatment with CoBLe-AgNPs was observed and reported by Jeyaraj et al. [40]. The content of phytochemicals in the extracts, such as

alkaloids, may be the main responsible for induction of apoptosis towards the cells by inducing caspase-3 mediated apoptosis. For example, it has been reported that alkaloids from *Angelicae dahuricae* can inhibit HeLa cell growth by inducing apoptosis through the caspase-3 pathway [41]. In an alternative manner, the cytotoxicity of our NPs may be partially due to the reactive oxygen species or through intracellular oxidative stress, triggering cell death by apoptosis and necrosis. Finally, the NPs exerting toxicity by transferring electrons from molecular oxygen or by blocking the electron transport chain (ETC) through an unknown mechanism may be one of the possible reasons for the potent cytotoxicity of *C. orchioides* in the nano-form. The reasons described above for the anticancer activity of the obtained AgNPs were supported by earlier reports on human cervical cancer cells [42]. In line with these studies, it is confirmed that the HeLa cancer cells treated with CoBLe-AgNPs showed an efficient growth inhibition rate.

Detection of Acridine Orange (AO) and Ethidium Bromide (EtBr) staining

On the basis of the overall cell morphology and cell membrane integrity, necrotic and apoptotic cells can be distinguished from one another using fluorescence microscopy (Fig. 5a–f). In the present study, it has been shown that the untreated

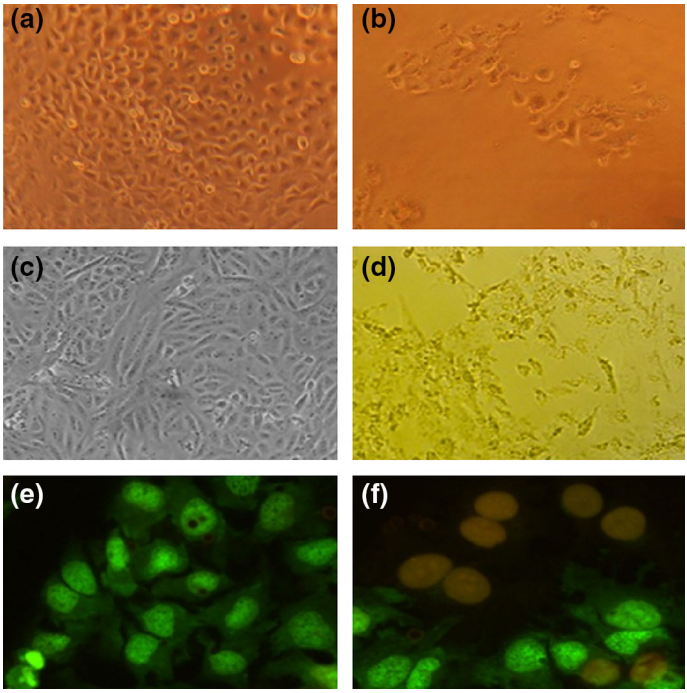

Fig. 5 Bright field and fluorescence microscopy images of HeLa and Vero *cell lines* treated with IC_{50} of CoBLe–AgNPs: **a** untreated HeLa cells; **b** HeLa cells treated with CoBLe-AgNPs; **c** untreated Vero cells; and **d** Vero cells treated with CoBLe-AgNPs. Fluorescence microscopy study of AO/EtBr stained HeLa cells: **e** control cells with *green colored* live images and **f** denotes the apoptotic cells with *orange color*

HeLa cells were stained with uniform green fluorescence, demonstrating viable cells in the untreated cell line. The percentage of total apoptotic cells was calculated in relation to their respective control cells. After treatment with the IC_{50} concentrations for a period of 48 h, the morphological changes were visualized. Orange apoptotic cells containing apoptotic bodies were observed (Fig. 5a–f). Apoptotic cells were observed as orange colored bodies due to nuclear shrinkage and blabbing. Similar results were also reported earlier in MCF-7, A549 and HepG2 cell lines by [42–44]. The percentage of apoptotic bodies obtained was 61% for the synthesized CoBLe-AgNPs.

Conclusions

Overall, a rapid protocol for the synthesis of AgNPs using aqueous leaf extracts of *C. orchioides* was reported using two simple production routes. The synthesized AgNPs were characterized by UV–Visible spectroscopy, XRD, and FTIR. Results confirmed the presence of various phyto-constituents, such as amides, aldehydes, ketones, alkynes and phenols, in *C. orchioides* aqueous leaf extracts. It was argued that these bioactive compounds were involved in the reduction of silver ions into metallic AgNPs. FESEM and HRTEM analyses highlighted the spherical morphology of the AgNPs. CoBLe-AgNPs have shown growth inhibition efficacy on *P. aeruginosa* (18 mm) and *S. aureus* (14 mm). The anti-proliferative activity of the *C. orchioides* AgNPs on the HeLa cancer cell line was investigated, and it was found that the AgNPs showed potential anticancer activity at a minimum concentration of 6.33 μg/mL. To the best of our knowledge, this is the first report on the synthesis of AgNPs using leaf extracts of *C. orchioides* and the evaluation of their efficacy on human pathogens as well as cervical cancer cells. Overall, the direct boiling of *C. orchioides* leaf extract shows excellent production of AgNPs as well as antibacterial and anticancer activities.

Acknowledgements The authors gratefully acknowledged Periyar University, Salem for providing UGC-Non-SAP, Research Fellowship, (Govt. of India) to T. Kayalvizhi. G. Benelli is sponsored by Regione Toscana PROAPI (PRAF 2015) and University of Pisa, Department of Agriculture, Food and Environment (Grant ID: COFIN2015_22). Founding sponsors had no role in the design of the study; in the collection, analyses, or interpretation of data, in the writing of the manuscript, and in the decision to publish the results.

References

1. R. Geethalakshmi and D. V. Sarada (2012). *Int. J. Nanomed.* **7**, 5375.
2. M. M. K. Abou El-Nour, E. Alaa, Al-W Abdulrhman, and A. A. A. Reda (2010). *Arabian J. Chem.* **3**, 135.
3. A. Majdalawieh, M. C. Kanan, O. El-Kadri, and S. M. Kanan (2014). *J. Nanosci. Nanotechnol.* **14**, 4757.
4. A. M. Pandian, C. Karthikeyan, M. Rajasimman, and M. G. Dinesh (2015). *Ecotoxicol. Environ. Saf.* **121**, 211.
5. P. Velmurugan, J. H. Park, S. M. Lee, J. S. Jang, K. J. Lee, S. S. Han, S. H. Lee, M. Cho, and B. T. Oh (2015). *J. Photochem. Photobiol. B* **147**, 63.

6. E. K. Elumalai, K. Kayalvizhi, and S. Silvan (2014). *J. Pharm. Bioallied Sci.* **6**, 241.
7. G. Benelli (2016). *Parasitol. Res.* **115**, 23.
8. G. Benelli (2016). *Enzyme Microb. Technol.* **95**, 58.
9. K. S. Nagesh and C. Shanthamma (2009). *Afr. J. Microbiol. Res.* **3**, 5.
10. N. Raaman, S. Selvarajan, C. P. Gunasekaran, V. Ilango, M. IIliyas, and G. Balamurugan (2009). *J. Pharm. Res.* **2**, 1272.
11. N. Soni, V. K. Lal, S. Agrawal, and H. Verma (2012). *Int. J. Pharm. Sci. Res.* **3**, 2407.
12. K. D. Arunachalam, L. B. Arun, S. A. Annamalai, and A. M. Arunachalam (2015). *Int. J. Nanomed.* **10**, 31.
13. G. McDonnell and A. Denver Russell (1999). *Clin. Microbiol. Rev.* **12**, 147.
14. J. A. Lemire, J. J. Harrison, and R. J. Turner (2013). *Nat. Rev. Microbiol.* **11**, 371.
15. M. Evander, K. Edlund, A. A. Gustafsson, M. Jonsson, R. Karlsson, E. Rylander, and G. Wadell (1995). *J. Infect. Dis.* **171**, 1026.
16. J. P. Shah and Z. Gil (2009). *Oral Oncol.* **45**, 394.
17. M. Abercrombie and E. J. Ambrose (1962). *Cancer Res.* **22**, 525.
18. X. J. Liang, C. Chen, Y. Zhao, and P. C. Wang (2010). *Methods Mol. Biol.* **596**, 467.
19. H. M. M. Ibrahim (2015). *J. Radiat. Res. Appl. Sci.* **8**, 265.
20. R. Sarada, V. Jagannadharao, and B. ShyamaSunder (2015). *Int. J. Eng. Res. App.* **5**, 82.
21. P. Velmurugan, S. Sivakumar, S. Y. Chae, J. S. Ho, Y. P. In, S. J. Min, and H. S. Chul (2015). *J. Ind. Eng. Chem.* **31**, 51.
22. P. Velmurugan, S. Sivakumar, Y. C. Song, and S. H. Jang (2015). *J. Ind. Eng. Chem.* **31**, 39.
23. N. S. Mewada, D. R. Shah, H. P. Lakum, and K. H. Chikhalia (2015). *J. Asso. Arab Univ. Basic Appl. Sci*. doi:10.1016/j.jaubas.2014.08.003.
24. V. D. Praveena and K. Vijaya Kumar (2014). *Indian J. Adv Chem. Sci.* **2**, 171.
25. T. Elavazhagan and K. D. Arunachalam (2011). *Int. J. Nanomed.* **6**, 1265.
26. K. D. Arunachalam, S. K. Annamalai, and S. Hari (2013). *Int. J. Nanomed.* **8**, 1307.
27. S. Saranya (2015). *Int. J. Phyto. Pharm.* **4**, 58.
28. J. Krithiga and M. BrigetMary (2015). *Pharm. Anal Acta* **6**, 427. doi:10.4172/2153-2435.1000427.
29. V. G. Kumar, S. D. Gokavarapu, A. Rajeswari, T. S. Dhas, V. Karthick, Z. Kapadia, T. Shrestha, I. A. A. RoyBarathy, and S. Sinha (2011). *Colloids Surf.* **87**, 159.
30. J. Polte (2015). *Cryst. Eng. Comm.* **17**, 6809.
31. P. R. Sajanlal, T. S. Sreeprasad, A. K. Samal, and T. Pradeep (2011). *Nano Rev.* **2**, 5883.
32. R. B. Malabadi, N. T. MetiGangadhar, S. Mulgund, K. Nataraja, and S. VijayaKumar (2012). *Res. Plant Biol.* **6**, 232.
33. P. Jena, S. Mohanty, R. Mallick, B. Jacob, and A. Sonawane (2012). *Int. J. Nanomed.* **7**, 1805.
34. A. Neumeyer, M. Bukowski, M. Veith, C. M. Lehr, and N. Daum (2011). *Nanomedicine* **7**, 410.
35. S. Rana and P. T. Kalaichelvan (2011). *Adv. Biotech.* **11**, 21.
36. A. E. Mohammed (2015). *Asian Pac. J. Trop. Biomed.* **5**, 382.
37. M. Serasanambati, S. R. Chilakapati, P. K. Manikonda, and J. R. Kanala (2015). *Int. J. Life Sci. Biotech. Pharm. Res.* **4**, 31.
38. N. Raaman, S. Selvarajan, C. P. Gunasekaran, V. Ilango, M. IIliyas, and G. Balamurugan (2009). *J. Pharm. Res.* **2**, 1272.
39. S. T. Aderonke, O. O. Selina, J. A. Babatunde, T. Mundi, and O. A. Magbagbeola (2013). *J. Biol. Sci.* **13**, 88.
40. M. Jeyaraj, G. Sathishkumar, G. Sivanandhan, D. Mubarakali, M. Rajesh, R. Arun, G. Kapildev, M. Manickavasagam, N. Thajuddin, K. Premkumar, and A. Ganapathi (2013). *Colloids Surf. B* **106**, 86.
41. Z. Han, J. Li, D. Gao, Z. Liu, and F. Zheng (2008). *Lab Med.* **39**, 540.
42. M. J. Firdhouse and P. Lalitha (2013). *Cancer Nanotechnol.* **4**, 137.
43. S. Z. Moghadamtousi, E. Rouhollahi, H. Karimian, M. Fadaeinasa, M. A. Abdulla, and H. A. Kadir (2014). *Drug Des. Dev. Ther.* **8**, 2099.
44. S. Z. Moghadamtousi, E. Rouhollahi, M. Hajrezaie, H. Karimian, M. A. Abdulla, and H. A. Kadir (2015). *Int. J. Surg.* **18**, 110.